Analysis of a Micro Grid Connected with a Solar Pond Using a Combination of Thermosyphon and Thermoelectric Modules

Faiz Mohd Siddiqui and V.K.Maurya*
Department of Electrical Engineering
BBD University, Lucknow, India.
*virendrakmaurya123@gmail.com

Abstract

A Solar pond is a pond containing salt water which used for storing solar thermal energy. This type of solar collector is cheap in construction and can store heat at higher temperatures in comparison to other types of solar collectors. A method of heat transference from lower zone to the hot surface of thermoelectric modules using gravity assisted heat pipes as thermosyphons is verified experimentally. The temperature difference of the lower convective zone and the upper convective zone is used upon the hot and cold surfaces of the thermo electric modules. An insulated solar pond with a surface area of 7 sq. m and a depth of 1.3 m was built to conduct performance experiments. From the results of experiment by using water as working fluid, the temperature of the solar pond in lower convective zone is at 50°C.It can be seen that the thermoelectric is able to generate electricity at 36 mV approximately. Usage of R134 a as a working fluid, the temperature of heat pond in lower convective zone is at 41°C.This has resulted in the generation of electricity at 234.25 mV. Research results in the present work have shown that there is a significant potential for power generation from small solar ponds through a simple and passive device incorporating thermosyphons and thermoelectric cells.

Keywords – Convective ,Thermosyphon, Raga, Thermoelectric , Solar Pond.

Introduction

Energy is vital for everyone's survival. We use energy in various forms over the year, which causes a number of significant power sources in the World to decline by the amount of time spent. Thus, many countries have started to look for alternative renewable energy to replace those that are vanishing. Many types of renewable energies such as wind power, hydro power, and biomass are brought in use. There is another type of renewable energy that is always available, inexhaustible, and not adversely affecting the environment. It is solar energy. The thermal efficiency of solar pond is increased by extracting heat from the gradient layer (Akbarzadeh *et al.,* 2005).

To use this energy, there must be a device that can store heat energy from the sun so that the stored energy can be utilized later for various usages. Solar pond is an option that can be used to collect heat from the sun due to its lower cost per square meter than other types of solar energy equipment (Akbarzadeh *et al.,* 2005).

Thus, here we have used the solar pond as a storing source of heat energy from the sun and used the thermosyphon heat pipe to transfer heat energy to the thermoelectric cells where electricity is generated from the temperature difference between the hot and the cold sides Electric power generation from solar

pond using combined thermosyphon and thermoelectric modules (Aliakba *et al.,* 2010).The heat energy is collected by heat pipes of thermosyphon which is then implemented in the Thermo electric generator for the generation of electric voltage (Rowe *et al.*, 1995).

Solar pond

Solar pond is a device to collect and store energy. It can operate continuously all year long. Solar ponds collect energy from solar radiation. The radiant heat is collected at the bottom side of the pond and this amount of heat would be used later. The structure of solar pond is shown in Figure 1. The size of pond depends on the usage of energy use such as water heating, crop drying, desalination, and electrical power generation. There is an amount of saline inside the pond. Generally, the saline solution is Sodium Chloride or Magnesium Chloride solution. The pond can be divided into three regions namely the surface zone, the insulation zone and the storage zone.

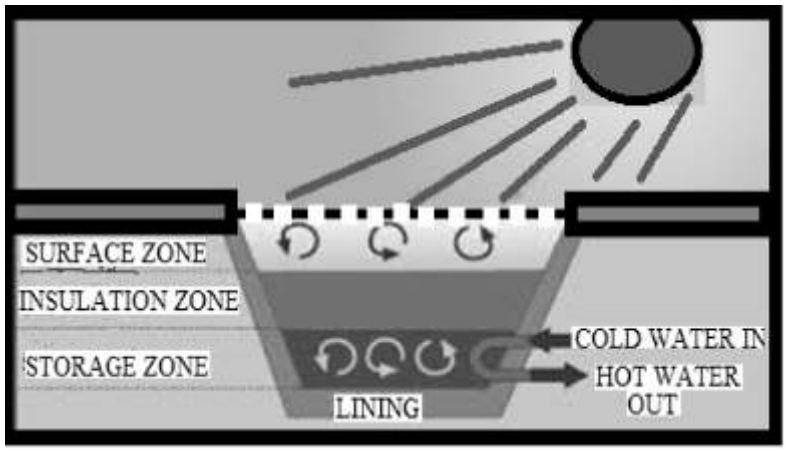

Figure 1: Solar pond

The surface zone is located at the top of the pond. The temperature of this zone is nearly closed to the surrounding temperature. The salt concentration is also near the clean water. Due to the contact between the surface layer of this zone and the surroundings, there is energy loss due to convection and evaporation. The next zone, non-convection or the insulation zone is below the upper convection zone. Here, the salt concentration is changed with the depth measured from the interface of the upper convective zone and non-convection zone. The increasing of depth from this interface results in the increasing of salt concentration. It function's to protect the heat convection from the optimum thickness of this zone yielding the high efficiency of energy storing inside the pond (Akbarzadeh *et al.,* 2005).

The last zone, storage zone, is the most salt-concentrated zone. The concentration in this zone is uniform. The pond, when receives heat from solar radiation, the heat penetrates through the upper and non-convection zone to be stored at the bottom side.

Thermosyphon

Thermosyphon is an effective heat transfer device that utilizes latent heat of the working fluid, flowing under the influence of gravity, to transport heat from the source to the sink. As the latent heat of

vaporization is relatively high, the thermosyphons can transfer large quantity of heat with very small end to end temperature differential and thus low thermal resistance (Tabor *et al.,* 1986).

$$Q_{oa} = \frac{\triangle T_{eff}}{Z_t} \quad (1)$$

Where, ΔT_{eff} [K] is effective temperature difference between heat source and sink and defined by:

$$\Delta T_{eff} = T_{so} - T_{st} - \Delta T_h \quad (2)$$

Here, T_{so} is the heat source temperature and T_{st} is the heat sink temperature and ΔT_h [K] is the mean hydrostatic temperature difference which is given as:

$$\Delta T_h = (T_p - T_v) F / 2 \quad (3)$$

Where F is the filling ratio and defined by:

$$F = V_l / A_{st} * L_e \quad (4)$$

V_l [m^3] is the volume of the working fluid, A_{ts} [m^2] is the internal cross section of the thermosyphon pipe and Le[m] is the evaporator length. T_p[K] the saturation temperature at the bottom of the pool is given by:

$$T_{p=} T_{v+}(L_e F * dTs / dH) \quad (5)$$

In the above equation T_v[K] is the temperature of the vapour in the adiabatic and condenser section T_s [K] is the saturation temperature of the boiling liquid and H[m] is the hydrostatic height of the liquid in the evaporator. The total thermal resistance – Z_t [K/W] from heat source to the heat sink for thermosyphon is related to the actual overall heat transfer - x oaQ [W] (Dunn *et al.,* 1981).

Figure 2: Thermosyphon

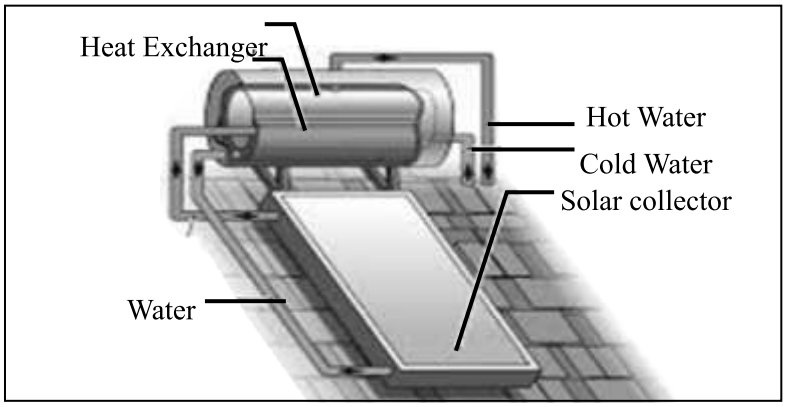

Figure 3(a) : Thermosyphon

An ideal network of thermal resistance of Z_1 to Z_{10} is shown in Figure 3.b. The individual thermal resistances as depicted in Figure 3 that make up the total thermal resistance from the heat source to the heat sink in the gravity assisted thermosyphon system is now discussed in detail (Dunn *et al.,* 1981).

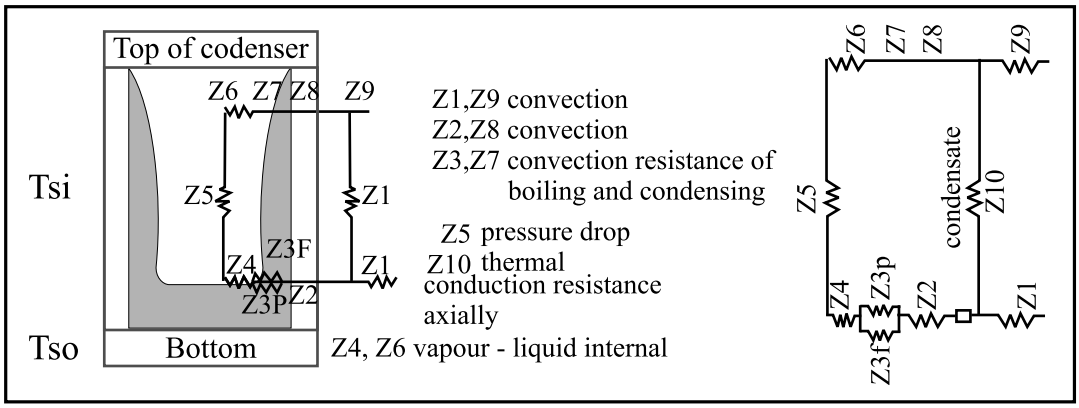

Figure 3(b): Thermal resistance and their location

Z_1 and Z_9 are thermal resistance between "heat source and the evaporator external surface" and "heat sink and condenser external surface" respectively. These can be expressed as:

$$Z_1 = \frac{1}{heoSco}$$
$$Z_9 = \frac{1}{hcoSco} \quad (6)$$

h_{eo},h_{co}[W/m^2.K] are evaporator and condenser outside heat transfer coefficient and s_{eo},s_{co}[m^2] are Evaporator and condenser external surface respectively (Faghri *et al.,* 1984).

Z_2 and $Z_8$are the thermal resistances present in the thickness of the thermosyphon tube wall in the "evaporative section" and "condenser section" respectively, which can be determined as

$$Z_2 = \frac{\ln(D_o/D_i)}{2\pi L_e k_p}$$
$$Z_8 = \frac{\ln(D_o/D_i)}{2\pi L_e k_p} \quad (7)$$

Where D_o, D_i [m] are external and internal diameters of the thermosyphon tube L_e,L_c [m] are evaporator and condenser length and K_p [W/m.k] is the thermal conductivity of the thermosyphon pipe material.

$Z_3$and Z_7 are the internal resistances due to pool and film boiling of the working fluid which

$$Z_{3p} = \frac{1}{\Phi_3 g^{0.2} Q^{0.4} (\pi D_i Le)^{0.6}} \quad (8)$$

Where, Φ3 [K-1] is the figure of merit for the case of pool boiling

$$\Phi_3 = 0.325 \left(\frac{p_l^{0.5} k_l^{0.3} C_{pl}^{0.7}}{p_v^{0.25} h_{vl}^{0.4} \mu_l^{0.1}} \right) \left(\frac{p_v}{p_a} \right)^{0.23} \quad (9)$$

Z_{3f} [K/W] is resistance from film boiling at the evaporator section:

$$Z_{3f} = \frac{CQ_0^{1/3}}{D_t^{4/3} g^{1/3} Le \Phi_2^{4/3}} \quad (10)$$

Where C is constant of the cylinder tube

$$C = \left(\frac{1}{4}\right)\left(\frac{3}{\pi}\right)^{\frac{4}{3}} = 0.235 \quad (11)$$

Where hv1[W/KG] is the latent heat of evaporation of the working fluid, K1[W/m.k] is the thermal conductivity of the working fluid in the liquid phase,ρ_l [kg/m3] is liquid density, ρ_v[kg/m3] is the vapour density,p_v[p_a] is the vapour pressure and p_a[p_a] is the atmospheric pressure. Z_4 and Z_6 are the thermal resistances that occur at the vapour liquid interface in the evaporator and condenser respectively (Faghri *et al.,* 1984). Z_5 is the effective thermal resistances due to the pressure drop of the vapour asit follows from the evaporator to the condenser.The value of Z_5 is quite small as compared to the value of Z_3 and Z_7. AS the magnitude of Z_4,Z_5,Z_6 and Z_{10} are negligible therefore these aregenerally neglected in the analysistherefore the overall thermal resistance is given by:

$$Z_t = Z_1+Z_2+Z_3+Z_7+Z_8+Z_9 \quad (12)$$

Thermoelectric Generator

In remote areas, where the electric grid is not available and the sun shines year round, combined power generation modules based on the small scale solar pond, thermosyphon and Thermo Electric Generator (TEG) is one of the viable candidates for providing daily electricity demand in such areas. A TEG has the advantage that it can operate from a low grade heat source such as waste heat energy. It is also attractive as a means of converting solar energy into electricity. The schematic diagram of the TEG is shown in Figure 3. It includes two dissimilar materials, n-type and p-type semiconductors, connected electrically in series and thermally in parallel to each other (Tabor *et al.,* 1986).

Heat is supplied at hot side at temperature T_{hs} while the other end is maintained at a lower temperature T_{cs} by a heat sink. As a result of the temperature difference, current I flow through an external load resistance Rex. The power output depends on the temperature difference, the properties of the semiconductor materials and the external load resistance.

For a TEG composed of n thermoelectric generating elements as shown by block diagram in Figure 3, the following parameters can be calculated and rate of heat supply is given by these equations:

$$Q_{hs} = \alpha I T_{hs} - 0.5 I^2 R_i + k_{teg}(T_{hs}.T_{cs})$$

Rate of heat removal

$$Q_{hs} = \alpha I T_{cs} - 0.5 I^2 R_i + k_{teg}(T_{hs}.T_{cs})$$

Output voltage

$$V = \alpha(T_{hs} - T_{cs}) - IR_i$$

Useful output power

$$P = \alpha I(T_{hs} - T_{cs}) - I^2 R_i$$

Each thermoelectric element is assumed to be insulated, both electrically and thermally, from its surroundings, except at the junction to hot/cold reservoir contacts.

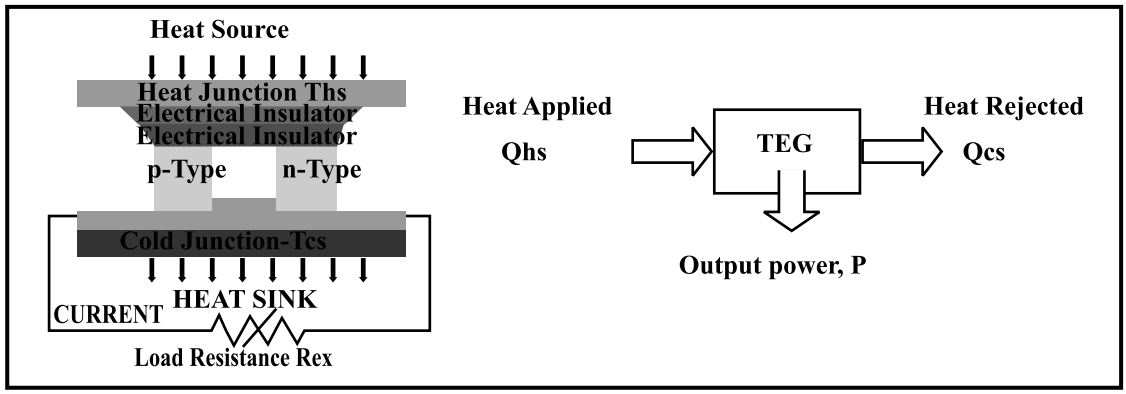

Figure 4: Schematic diagram of TEG.

The internal irreversibility for the TEG is produced by Joule electrical resistive loss and heat conduction loss through the semiconductors between the hot and cold junctions. The Joule losses generate internal heat equal to I2Ri where I [A] is electric current generated by thermoelectric generator, Ri [Ω]is the total internal resistance of the thermoelectric generator. Conduction heat loss is kteg (Ths - Tcs) where, kteg [W/m.K] is thermal conductivity of thermoelectric generator. The external irreversibility is caused by finite rate heat transfers at the source and the sink (Singh *et al.,* 2011). For a TEG composed of n thermoelectric generating elements as shown by block diagram in Figure 4, the following parameters can be calculated (Tabor *et al.,* 1986).

Experimental Set Up

This experiment was made into two sets. The first set of experiment was carried out in the lab to determine the correct thermal performance of the heat pipe in drawing heat from the solar pond before the best values were taken to create an experiment kit to be installed later in the solar pond.

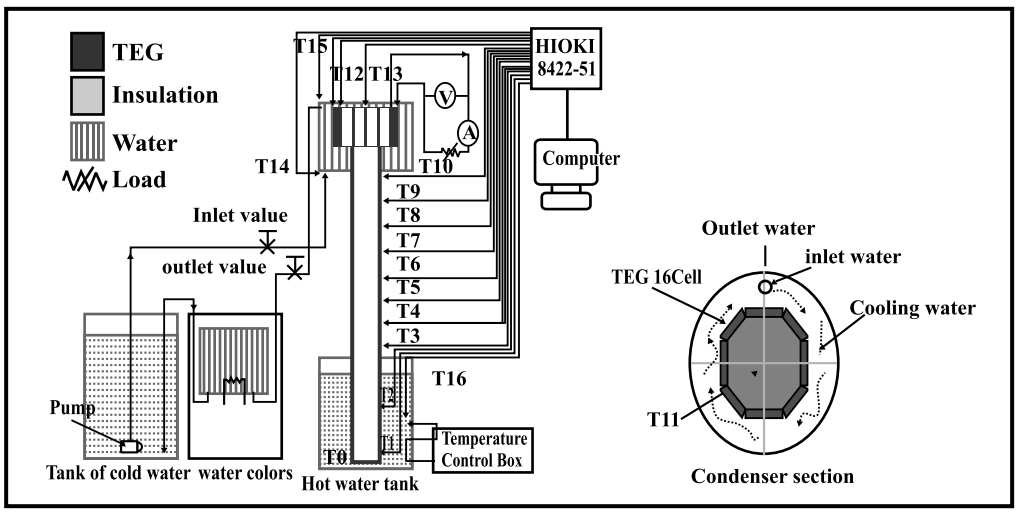

Figure 5: Schematic Combined thermosyphon and thermoelectric modules

The heat pipe was made from a copper tube with an external diameter of 0.54 m. The length of the evaporation section, the heat insulation section, and the condensation section are 0.3, 0.93, and 0.09 m. respectively. Heater was used to heat the water in the evaporation section by controlling the temperature of water from 40 to 100 °C and the temperature was increased every 10 °C. Heat at the condensation section was vented by cooling water from the cooler EYELA CA -1112CE with an error in measurement of +2 °C (Tabor *et al.,* 1986).

The flowing rate of water was adjusted at 0.02374 kg/s. Two K-type thermocouples with an error in measurement of +0.5 °C were mounted on the heat pipe of the evaporation section, eight were mounted on the heat insulation section and another three were in the condensation section respectively in order to measure the heat distribution in different positions of the heat pipe. The thermocouples were also mounted at the entrance and exit of the cooling water in the evaporation section in order to calculate the heat transfer of the heat pipe. Data were collected every 10 minutes by using a temperature recorder HIOKI 8422-51 +0.1 °C. Sixteen thermoelectric cells were installed at the condensation section of the heat pipe. An Ampere Meter and a Voltmeter were mounted to measure the voltage and the electric current generated by the thermoelectric cell (Singh *et al.,* 2011).

Results and Discussion

Laboratory Testing and Results

Figure 6 showed the distribution of temperature on the length of the heat pipe. To observe its performance in transferring the heat, the pipe was divided into three parts; the evaporation section, the heat insulation section, and the condensation section with 0.30, 0.93, and 0.09 m. in diameter respectively. Here, the rate of flow of cooling water was controlled at 0.02374 Kg/s. The temperature of cooling water at the condensation section was 10 °C. The results showed that when the temperature at the evaporation section increased, heat transfer of the heat pipe increased accordingly as the evaporation section received much heat hence making the working fluid inside the heat pipe change its status into steam moving to transfer more heat at the condensation section. This could be noticed that when the temperature at the evaporation section increased, the temperature at the condensation section was similar to that of the evaporation section. When the temperature at the evaporation section was over 70 °C, the rate of heat transfer decreased when compared to the increased temperature in the evaporation section. It was due to the insufficient working fluid moving to fill the evaporation section but was blocked by the vapour bubbles that were moving to cool the condensation section. In the experiment, the right temperature at the evaporation section had a good rate of heat exchange at 70 °C.

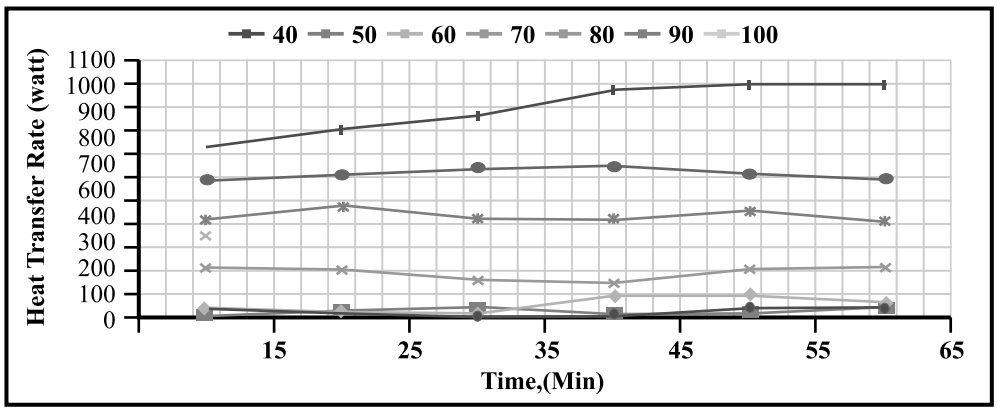

Figure 6: The distribution of temperature on the length of the heat pipe

Figure 7 (a) showed the heat transfer of the heat pipe. The heat transference at the condensation section was calculated by using Calorific value by increasing the temperature at the evaporation section by 10 °C each time from 40 to 100 °C. From Figure 8, the rate of heat exchange changed according to heat values at the evaporation section. When the temperature at the evaporation increased, the heat transfer changed accordingly. At the beginning of experiment, the heat transfer slowly increased as the working fluid changed its status into steam to transfer heat at the condensation section (Rowe *et al.,* 1995).

As time increased, the rate of heat exchange also increased and would become stable when the heat pipe got into its stable status. The results revealed that when the heat transfer became constant and consistent, the temperature at the evaporation section was at 90 °C (temperature difference).

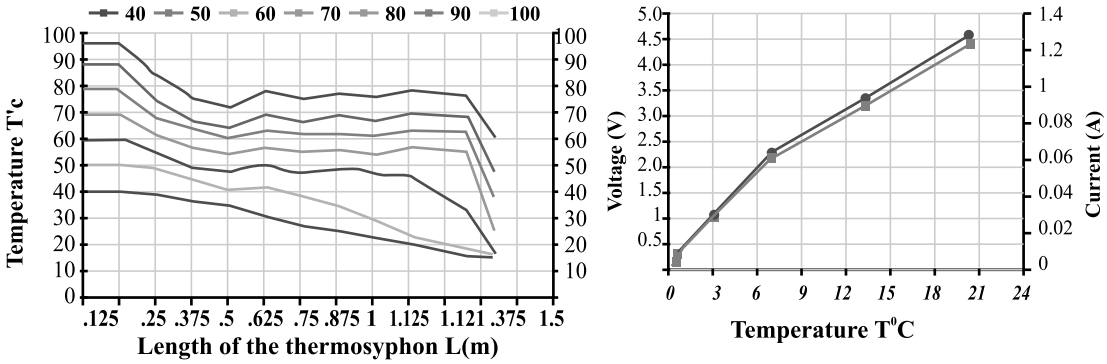

Figure7(a): The relation heat transfer rate of thermosyphon versus time

(b) : The relation between the hot and the cold sides versus electric generated by the thermoelectric cells.

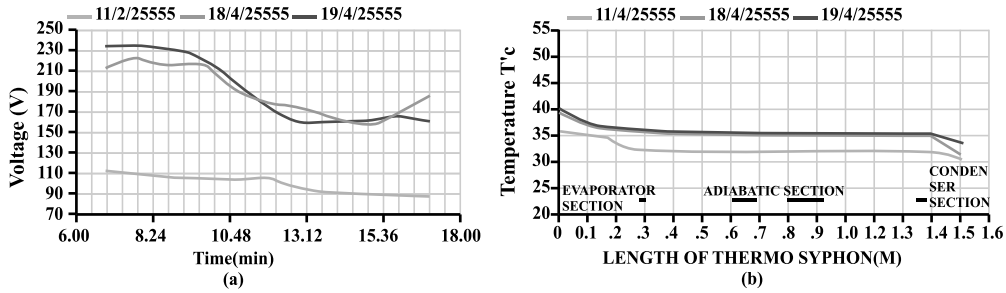

Figure 8(a): The relation between the Temperature versus the length of Themosyphon

(b) The relation between the electric current generated by the thermoelectric cells versus time

Figure 8 (a) showed the relation between the temperature of the thermo syphon pipe and the length of the heat pipe. The experiment was conducted three times. The first experiment was carried out with the temperature of under heat convection at 35.9 °C, the green curve, the temperature for evaporation at 33 °C, the temperature for condensation at 30.9 °C, and the temperature difference between the two sides at 2.1 °C. The second experiment was conducted by using the temperature of under heat convection at 38.7°C, the temperature for evaporation at 36.6 °C, the temperature for condensation at 31.6 °C, and the temperature difference between the two sides at 5 °C. Finally, the third experiment showed that the temperature difference between the two sides was 3.38 °C. It is observed from the figures that the heat pipe could draw heat from the evaporation section to transfer heat at the condensation section without the change of temperature at the heat insulation section (Aerodromnaya *et al.,* 1973).

Figure 8 (b) showed the relation between the voltage and the time. From this figure, it could be seen that the voltage generated by the thermoelectric cells changed according to the time and the temperature difference of the two sides of the heat pipe. It is observed that the temperature on the hotter side of the thermoelectric cells was dependent on the temperature of the under heat convection layer of the solar pond whereas the temperature on the cold side was dependent on the temperature of the upper heat convection layer of the solar pond. From the red and blue curves, it could be seen that at 07:00 hr., the generated voltage increased and would decrease when the temperature in the upper heat convection layer increased and the voltage would increase when the temperature in the under heat convection layer increased at 15:00 hr.

Table-1: Major Salt – Gradient Solar Ponds (In India)

Location	Area(m^2)	Depth(m)	Main Objective	Achievements
Bhavnagar (India)	1210	1.2	Operating experience and behaviour of materials	Max. Temp 34 Celsius 2972 working for two years
Bhavnagar (India)	1000	2.3	Operating experience and applications for power production	Getting heated, designed to supply 20KW.
Puducherry (India)	100	2.0	Experience material behaviour, monitoring and modelling.	Built in 1989

Conclusion

This article suggests that installing the thermosyphon heat pipe in the solar pond to draw heat from the heat convection layer and transfer it to the thermoelectric cells is appropriate. The voltage generated by the TEG is dependent on the temperature difference between the hot and the cold sides of the thermoelectric cells. When the difference very varies, the thermoelectric cells can generate much voltage. The temperature difference of the two sides is also dependent on the temperature of the under heat convection layer which acts as a heat source for the thermosyphon heat pipe. And the temperature at the upper heat convection acts also as a heat transfer for the thermoelectric cells (as demonstrated in the experiment at 07:00 hr. where the highest voltage of 234.25 mill volts was generated and was slowly decreasing later as the temperature at the upper heat convection layer increased from 30 to 34 °C resulting in less temperature difference between the two sides and hence making the thermoelectric cells generate less voltage accordingly.

Acknowledgements

This research was financially supported by parents of Faiz Mohd Siddiqui. Authors thank to Mr. Manish Singh & Mr. Rakesh Sharma, Assistant Professor, Electrical Engineering, BBD University, Lucknow for their support & guidance.

References

Akbarzadeh, A., Andrews J., and Golding P. 2005. Solar Pond Technologies: A Review and Future Directions, Chapter 7, *Advances in Solar Energy, EARTHSCAN*. 233-294.

Andrew J., Akbarzadeh A., 2005. Enhancing the thermal efficiency of solar pond by extracting heat from

the gradient layer, *Solar Energy.*78 (1), 704 -716.

Dunn, P. D., Reay, D. A. 1994. Heat Pipes, Pergamon, Fourth Edition , Oxford ,England.

Engineering Sciences Data sheet 81038. 1981. Heat Pipe-performance of Two-Phas Closed Thermosyphon. *Engineering Sciences Data Unit ESDU*, London.

Faghri, A. 1985. Heat Pipe Science and Technology, DC, *Taylor & Francis*. 160-161.

Ha, B. 1984. Ormat Turbines, Arava Solar Pond Inaugurated*, Sunworld*. 8(1) 18-25.

Tabor, H., Doron, B. 1986. Solar Ponds- Lessons learned from the 150 kW(e) power plant at Ein Boqek, *Proc. of the ASME Solar Energy Div., Anaheim, California*.

Singh, R., Tundee, S., Akbarzadeh, A. 2011. Electric power generation from solar pond using combined thermosyphon and thermoelectric modules. Mechanical and Manufacturing Engineering, RMIT University, *Solar Energy.* 85(1),371 -378.

Rowe, D. 1995. M.CRC Handbook of Thermoelectrics, CRC Press.

KRYOTHERM, 6 Aerodromnaya Street, Saint-Petersburg, 1973, Russia, Tel.: (812) 394-1310, Email: info@kryotherm.ru http;//www.kryotherm.